Environmentally Relevant Atrazine Exposure Leads to Increases in DNA Damage and Changes in Morphology in the Hepatopancreas of Crayfish (Faxonius Virilis)

Rachelle Belanger (belangra@udmercy.edu)
University of Detroit Mercy https://orcid.org/0000-0003-3902-9276
Mohammad Hadeed
University of Detroit Mercy
Carlie Castiglione
University of Detroit Mercy
Diana Chammout
University of Detroit Mercy
Karen Crile
University of Detroit Mercy
Sara Abdulelah
University of Detroit Mercy
Ebrahim Rampuri
University of Detroit Mercy
Gregory Grabowski
University of Detroit Mercy
Ali Maalhagh-Fard
University of Detroit Mercy
Sayf Saleem
University of Detroit Mercy

Research Article

Keywords: Crayfish, atrazine, DNA damage, morphological changes, tubular degeneration, vacuolization

Posted Date: March 3rd, 2022

DOI: https://doi.org/10.21203/rs.3.rs-1408998/v1

Abstract

Exposure to the herbicide atrazine at environmentally relevant concentrations has been shown to negatively impact aquatic organisms, including crayfish. Because xenobiotics are concentrated in the crayfish hepatopancreas (digestive gland), we examined changes in morphology and DNA damage in hepatopancreatic tissue structure and cells following a 10-day exposure to atrazine (0, 10, 40, 80, 100 and 300 ppb). We found that there were marked morphological changes, post-exposure, for all atrazine concentrations tested. Hepatopancreatic tissue exhibited degenerated tubule epithelium with necrosis of microvilli, tubule lumen dilation and vacuolization of the epithelium. These changes increased in a dose-dependent manner. Likewise, we also performed a terminal deoxynucleotidyl transferase (TdT) mediated dUTP nick-end labeling (TUNEL) assay which showed the percentage of cells with DNA damage increased following atrazine exposure. Crayfish hepatopancreatic tissue displayed significant increases in TUNEL-positive cells following exposure to atrazine at 100 ppb and above. Overall, exposure to atrazine at environmentally relevant concentrations damages hepatopancreatic tissue, leading to an inability to detoxify atrazine and a potential to bioaccumulate atrazine long-term.

Highlights:

- DNA damage to hepatopancreas cells increased following exposure to atrazine.
- Atrazine exposure leads to morphological changes in hepatopancreas lobules.
- Tubular epithelium degeneration increased as atrazine concentrations increased.
- Vacuolization of the hepatopancreas lobules increased following atrazine exposure.

Introduction:

Herbicides are heavily used in agricultural areas to control unwanted plant growth and subsequently increase crop yields. Atrazine (ATR; 2-chloro-4-ethylamino-6-isopropylamino-1,3,5-triazine) is a chlorotriazine herbicide and is one of the most heavily applied herbicides in the United States (U.S.) with over 32 million kg being applied annually (EPA, 2020). ATR is typically applied to corn, sorghum and sugarcane crops to control the growth of broad leaf weeds. After being applied to agricultural areas, ATR can enter local streams and rivers through run-off, ground water seepage, regional transport (evaporation) and may be deposited by rain water (LeBlanc et al., 1997; Tong and Chen, 2002). Although the U.S. Environmental Protection Agency (EPA) sets a limit of 15 µg/L (ppb) ATR (60-day average) and an in-field downwind buffer of 4.6 m from aquatic environments, ATR has been detected at levels above 300 ppb in some U.S. rivers (EPA, 2014; Belanger et al., 2016; EPA, 2020). These elevated concentrations have also been shown to last for several weeks during the spring season (EPA, 2014). Exposure to high concentrations of ATR is also compounded by the fact that the half-life of ATR ranges from six days to several months or years (Comber, 1999). ATR has also been detected for up to 22 years following its application due to its potential for soil sorption and high soil mobility (Walther, 2003; Jablonowski et al.,

2011). This is of concern because ATR exposure can then have long-term impacts on non-target species, like aquatic organisms, for years.

Understanding the impacts of ATR exposure on non-target aquatic organisms has been the focus of many reviews (Giddings, 2005; Solomon et al., 2008; Van Der Kraak et al., 2014; de Albuquerque et al., 2020). Because ATR comes into contact with a broad range of aquatic organisms, it can cause sublethal effects to nontarget species and interfere with the behavior, morphology and physiology of many species at environmentally relevant concentrations. ATR has been shown to affect reproductive physiology and behavior. For example, acute exposure to ATR led to demasculinization and feminization of male frogs (*Xenopus laevis*), feminization of mussels (*Elliptio complanata*), altered sperm quality in zebrafish (*Danio rerio*) and an inability to detect and localize mate odors in crayfish (*Faxonius rusticus*) (Tavera-Mendoza et al., 2002; Hayes et al., 2003; Flynn et al., 2013; Belanger et al., 2017a; Bautista et al., 2018). Gunkel and Streit (1980) suggest that ATR enters the body of most aquatic organisms via the gills and can be concentrated in various organs and tissues. ATR has been shown to accumulate in the liver/hepatopancreas, gallbladder and ovaries in fish (*Danio rerio*, *Tilapia sparrmanii, Coregonus fera, Cyprinus carpio*) and in the visceral mass, foot and mantle of bivalves (*Ancylus fluviatilis, Anodontites trapesialis* and *Corbicula fluminea*) following an acute exposure (Gunkel and Streit, 1980; du Preez and Van Vuren, 1992; Jacomini et al., 2006; Xing et al., 2012; Al-Sawafi and Yan, 2013). ATR was also shown to cause DNA damage in cells of tissues where it is known to accumulate. Exposure to ATR causes biochemical changes and DNA damage in the cells of the hepatopancreas of *D. rerio* and liver of *Prochilodus lineatus* (Zhu et al., 2011b; Santos and Martinez, 2012). DNA damage was also detected in peripherally located antennule cells of crayfish (*Faxonius virilis*) following acute ATR exposures (Abdulelah et al., 2020). Because of where they are located, these appendages and cells presumably come in contact with ATR readily in their environment, leading to damage and long-term chemosensory deficits (Belanger et al., 2016). Changes in morphology, in addition to the expression and activity of detoxification enzymes and antioxidant biomarkers of the hepatopancreas (digestive gland) of crayfish (*F. virilis*, *Procambarus fallax f. virginalis*, *Cherax destructor*), were also noted following exposure to ATR and its metabolites (Velisek et al., 2017; Stara et al., 2018; Steele et al., 2018; Awali et al., 2019). Many invertebrates, including crayfish, rely heavily on the hepatopancreas for detoxification of xenobiotics following exposure.

The hepatopancreas of the crayfish serves as the main energy reserve for growth and molting. Additionally, it is the main site of digestion, absorption and storage of nutrients. It is also the main organ of detoxification of xenobiotic compounds (Holdich, 2002). Given that the central function of the hepatopancreas in crayfish is the digestion of food and protection of the body from toxins, the physical, physiological and morphological state of this organ can provide insights into the effects of xenobiotics (for review see Belanger et al. (2017b)). Crayfish hepatopancreatic tissue can be used to monitor the health of the crayfish and can indicate when the animal has been exposed to harmful substances (Xiao et al., 2014; Velisek et al., 2017). Following exposure to xenobiotics, the hepatopancreas bioaccumulates by storing them in intracellular vacuoles (Icely and Nott, 1992). Changes in the histological organization of the crayfish hepatopancreas may be used as a bioindicator of contamination (Popescu-Marinescu et

al., 1997; Desouky et al., 2013; Koutnik et al., 2014; Stara et al., 2016; Belanger et al., 2017b; Stara et al., 2018; Laurenz et al., 2020). The hepatopancreas is formed by numerous tubules separated by connective tissues with four types of epithelial cells, including blister-like secretory cells (B cell) which form large vacuoles that channel off harmful substances (Abd El-Atti et al., 2019). Further, these large vacuolar structures have been recognized as secondary lysosomes that are involved in enzymatic breakdown of xenobiotics and in cellular autophagy (Brown, 1982). Given the importance of the hepatopancreas in detoxification, its morphology and physiology can be used to identify areas of the aquatic environment that are under the stress of pollution.

In this study, we investigated whether exposure to environmentally relevant concentrations of ATR (0, 10, 40, 80, 100 and 300 ppb) for 10 days caused morphological and cellular changes in hepatopancreas of crayfish. We hypothesized that as the exposure concentration increased, there would be changes in the morphology of the lobules of the hepatopancreas. Our hypothesis is based on studies indicating deterioration of the tubular epithelium and vacuolization of the hepatopancreatic lobules following exposure to the herbicides metolachlor and prometryne, and to pyrethroid insecticides (Wei and Yang, 2015; Stara et al., 2018; Stara et al., 2019). Moreover, because ATR exposure was shown to cause significant DNA damage, we also expected to see dose-dependent increases in hepatopancreatic cells with DNA damage following exposure to ATR (Liu et al., 2006; de Campos-Ventura et al., 2008; Cavas, 2011; Zhu et al., 2011b; Santos and Martinez, 2012; Abdulelah et al., 2020). To investigate DNA damage, we used a TdT mediated dUTP nick-end labeling (TUNEL) assay. In support of our hypothesis, we expected the percentage of TUNEL-positive cells in the hepatopancreas to increase in a dose-dependent manner. Additionally, we also expected to see an increase in vacuolization, tubular destruction and a decrease of microvilli in the hepatopancreas with increasing detoxification of ATR. Overall, it is important to understand how ATR-induced changes affect the morphology of the hepatopancreas, as overall physiological function is correlated with physiological condition (Popescu-Marinescu et al., 1997). Acute ATR exposure could lead to long-term changes in the crayfish's ability to detoxify xenobiotics and subsequently affect survival.

Materials And Methods:

Animals:

Male and female *Faxonius virilis* crayfish (weight: 27.0 ± 10.3 g, carapace length: 4.4 ± 0.6 cm, chelae length: 3.8 ± 0.8 cm; mean ± standard deviation, N = 18), used in this experiment, were collected from Belle Isle Park and William G. Milliken State Park (Detroit, MI) using bated traps. There was no difference in the size of crayfish used for each of the concentrations tested (one-way ANOVA; $F_{5,17} = 3.10$; $p = 0.81$). They were housed at the University of Detroit Mercy in large tanks [mean water chemistry parameters: pH 7.5, dissolved oxygen = 8.29 mg L^{-1}, dissolved oxygen percent saturation = 96.45%, temperature = 22.3 °C, hardness = 250 ± 25 mg L^{-1}, and TOC = 2.54 mg L^{-1}; 14:10 h light dark cycle] for at least two weeks prior to treatments. During this time and throughout the treatments, crayfish were fed one rabbit pellet per crayfish three times per week.

Atrazine Treatments:

Atrazine treatments were performed using methods from Abdulelah et al. (2020). Crayfish were treated for 10 days in 3000 mL translucent plastic containers (31 cm length ± 18.5 cm width ± 11 cm height; N = 1 crayfish per container) with secured lids. Each container was filled with control or ATR-treatment and aerated using an air stone (N = 3 crayfish per treatment). Stock ATR was prepared using the methods from Abdulelah et al. (2020) where 17 mg of ATR (Sigma-Aldrich, 99.1% purity) was dissolved in 2.5 mL of 100% ethanol using a vortexer. This mixture was then diluted with 997.5 mL of distilled water (final concentration of stock 17 mgL^{-1}). Stock ATR was added to each container to reach the final environmentally relevant ATR concentration desired (10, 40, 80, 100 and 300 ppb). Control crayfish were treated 0 ppb ATR (final ethanol concentration of 0.004%). Reversed-phase liquid chromatography-tandem mass spectrometry (LC/MS) analysis was performed to verify and standardize all ATR solutions (see Table S1 in Awali et al., 2019).

Tissue Collection, Processing and Staining:

Following treatment, crayfish were placed in a -20 ℃ freezer for 10–15 min before being decapitated. The hepatopancreas was removed by making a ventral incision in the abdomen with scissors and the hepatopancreas was subsequently weighed. Once the hepatopancreas was isolated, it was cut into 0.5 cm cubes and placed in labeled falcon tubes containing 4% paraformaldehyde (PFA) at 4 ℃ for at least 48 h. Following fixation, hepatopancreas tissues were prepared for paraffin embedding by treating tissues with 50%, 75%, 95% and 100% ethanol, 100% xylene and paraffin (15 min; three replicates). Hepatopancreatic tissue was embedded in a paraffin mold and allowed to cool. The molds were placed in the freezer overnight to fully solidify the paraffin blocks (Bancroft and Stevens, 1990). Paraffin-embedded blocks were sectioned (5 μm) using a microtome (Microm HM 325A, Waldorf, Germany) and floated on a water bath. Sections were subsequently collected on microscope slides and dried on a slide warmer.

Serial sections were stained with hematoxylin and eosin (H&E) to determine if ATR exposure caused changes in morphology and a terminal deoxynucleotidyl transferase (TdT) mediated dUTP nick-end labeling (TUNEL) assay was also used to examine if DNA damage also occurred. For H&E staining, a standard procedure was followed where sections were deparaffinized with xylene, rehydrated using a descending ethanol series, stained with hematoxylin (5 min), decolorized, counterstained with eosin (10 min), dehydrated with 95% (1 min; 1 replicate) and 100% ethanol (1 min; 3 replicates), cleared with xylene (1 min; 3 replicates) and mounted with Permount (Bancroft and Stevens, 1990). H&E sections were imaged using a Nikon Eclipse light microscope with a DAGE-MTI colored camera (Tokyo, Japan).

Hepatopancreas sections were also examined for DNA damage using a TUNEL assay (ApopTag Plus Peroxidase *In Situ* Apoptosis Detection Kit, S7101; EMD Millipore Corp., Temeculla, CA). This technique uses TdT to catalyze template-independent addition of digoxigenin-dUTP and dATP to 3' OH ends of fragmented DNA. The incorporated nucleotides form a heteropolymer of digoxigenin-dUTP and dATP, and an antidigoxigenin antibody conjugated to peroxidase is then added and subsequently visualized. This

assay was performed following manufacturer's instructions. Briefly, sections were deparaffinized, rehydrated and incubated with proteinase K (60 µg/mL) for 15 min at 37°C. Sections were then washed in distilled water and treated with 3% hydrogen peroxide in 0.1 M phosphate buffered saline (PBS) for 5 min at room temperature to quench endogenous peroxidase activity. A mixture containing digoxigenin-conjugated nucleotides and TdT was applied to the sections in a humidified chamber (37°C for 1 h). Sections were then treated with antidigoxigenin-peroxidase for 30 min at room temperature in a humidified chamber and substrate-chromogen mixture for 5 min. Sections were then stained with 0.25% methyl green that was heated and filtered before the stain was applied for 5 min and rinsed in distilled water. Mounting medium (VECTASHIELD with 4',6-diamidino-2- phenylindole (DAPI), Vector Labs) was added to the slides, coverslips were applied and sealed with clear nail polish. Negative and positive controls were performed using hepatopancreas tissue from control crayfish. For the negative control, hepatopancreas sections were processed in an identical manner, however distilled water was used as opposed to the TdT enzyme. For positive controls, DNase was applied to the hepatopancreas tissue for 10 min following proteinase K treatment. Color images were visualized using the same microscope as H&E sections. To evaluate the percent TUNEL-positive cells, slides were also imaged using both light and fluorescence microscopy (Zeiss Axio Scope.A1). Nuclei of the cells fluoresce blue after being exposed to UV light due to DAPI which labels nuclei. Subsequently, a black and white image of the same section was also obtained and TUNEL-positive cells were identified from a black and white binary image where the black spots represented candidate cells that were positive in both the DAPI and TUNEL channels (Heisler-Taylor et al., 2018).

Data Collection and Statistical Analysis:

H&E images were examined and changes in hepatopancreas pathological features including examination of the tubular epithelium, vacuolization and cellular morphology were analyzed and compared for both control and ATR-treated crayfish (Desouky et al., 2013; Stara et al., 2018). To examine the effects of ATR on DNA damage in hepatopancreas, ten images of TUNEL-positive cells (cells that were both black and DAPI-positive) and DAPI-positive cells were obtained from each animal. Each image (22.6 mm^2) was evaluated to determine the percentage of cells that were TUNEL positive. Ten representative sections were imaged from each crayfish hepatopancreas. TUNEL-positive and DAPI-positive cells from a 22.6 mm^2 area of each section were counted. Cells were counted using Cell-Counter, a Fiji plugin (Muñoz de Toro et al., 1998; Abdulelah et al., 2020). The average number of cells counted (± standard error (SE)) in each image was 178.7 ± 5.8 cells. The percent TUNEL-positive cell data was obtained by dividing the total number of TUNEL-positive cells by the total number of DAPI-positive cells and multiplying by 100 for each image. Percentages were subsequently arcsine transformed. A linear mixed models method followed by analysis of deviance tables using Type III Wald v2 tests with Satterthwaite's method (Zuur et al., 2009) were used to determine the effect of concentration on the presence of TUNEL-positive cells in the lme4 package in R statistical software (Bates et al., 2015; R Development Core Team, 2019). Differences of least squares means ('difflsmeans') from the lmerTest package in R was used as a post hoc test to discern which concentrations were significantly different from each other (Kuznetsova et al.,

2017). Fixed factors include concentration and length of exposure and random factors include TUNEL-positive cell counts from individual crayfish.

Results:

Histopathology:

Histological examination of hepatopancreas lobules was performed following 10-day ATR exposures. In control crayfish, the lobules were well organized, unbroken and uniform with asterisk-like lumens. An intact microvillar brush border was apparent in all sections examined. Many small lipid vacuoles were observed in the lobules with very few B cells containing large vacuoles (Fig. 1A). The hepatopancreas of crayfish exposed to ATR exhibited degenerated tubule epithelium with necrosis of microvilli, tubule lumen dilation and vacuolization of the epithelium (Fig. 1B-F). Pronounced disintegration of the microvilli brush border as well as the presence of B cells containing large vacuoles increased in hepatopancreas lobules in a dose-dependent manner. Moreover, the lumen of the lobules of crayfish treated with ATR became less organized, contained irregular and damaged epithelia, lost their asterisk-like shape and became more dilated. The lipid vacuoles were reduced in size and number following all ATR exposures.

[Insert Fig. 1]

DNA Damage:

Examination of DNA damage was done using a TUNEL assay which labeled the nuclei of cells with DNA damage a black-brown color. The hepatopancreas of control crayfish, treated with 0 ppb ATR, contained very few TUNEL-positive nuclei (Fig. 2A). Following ATR exposure, increases in TUNEL-positive cells can be visualized in all tissue sections (Fig. 2B-F). The number of TUNEL-positive cells increased with increasing ATR exposure concentrations following 10-day exposures ($F_{5,72,0.05} = 3.46$, $P < 0.0001$; linear mixed-model with Satterthwaite's method; Fig. 3). Control crayfish (0 ppb ATR), had 5.7 ± 0.6% (average ± SE) TUNEL-positive cells present in representative sections of 22.6 mm^2 of hepatopancreas tissue. Following exposure to 10, 40 and 80 ppb ATR, 9.3 ± 0.9%, 15.1 ± 1.8% and 14.9 ± 2.3% TUNEL-positive cells were visualized respectfully. There was a significant increase in TUNEL-positive cells seen following 10-day exposures to 100 and 300 ppb ATR ($p < 0.01$ when compared to the 0 ppb ATR treatment). Following an exposure to 100 and 300 ppb ATR, 33.5 ± 5.8% and 32.6 ± 1.7% TUNEL-positive cells were present (Fig. 3).

[Insert Fig. 2]

[Insert Fig. 3]

Discussion:

A properly functioning hepatopancreas is essential for digestion, growth, molting and detoxication of xenobiotics. When crayfish are exposed to ATR, enzymes such as cytochrome P450 and glutathione-S-transferase detoxify it by producing more water-soluble metabolites that can easily be excreted from the body (Brzezicki et al., 2003). If the hepatopancreas is damaged, crucial functions are severely inhibited. Our data show that when crayfish are exposed to ATR for 10 days at environmentally relevant concentrations, hepatopancreatic tissue degenerates in a dose-dependent manner. More specifically, the lobule morphology is altered and necrosis of the microvillar brush border is evident (see Fig. 1). Blister-like cells with large vacuoles can also be seen following all ATR exposures tested. Moreover, an increase in DNA damage in over 30% of cells of the hepatopancreas following exposures to 100 and 300 ppb ATR is evident (See Figs. 2 & 3). This is significant because environmental exposures to ATR have been found at concentration exceeding these exposures and thus exposure concentrations above 100 ppb can have profound effects on the ability of the hepatopancreas to function effectively (Graymore et al., 2001; EPA, 2014; Belanger et al., 2016).

Exposure to xenobiotics such as ATR can have many negative impacts on the morphology, physiological processes and biochemical pathways in aquatic organisms, like crayfish (Belanger et al., 2017b). In crustaceans, there is a link between the physiological condition of the animal and the structure and morphology of the hepatopancreas (Popescu-Marinescu et al., 1997). Acute ATR exposures altered the morphology of the hepatopancreas at all concentrations tested. Structural changes were noted following exposures to ATR concentrations as low as 10 ppb. Following a 10-day exposure to 10 ppb ATR, we saw changes to the hepatopancreas tubules including degeneration of the microvillar brush border and vacuolization of secretory B (blister-like) cells. These pathologies increased as ATR exposure concentrations increased. For example, the epithelium lining the lumen of the lobules was almost completely degenerated at exposure concentrations over 100 ppb. Further, there was also an increase in tubule lumen dilation, which is also an indication of tissue atrophy. Vacuolization of the secretory B cells also increased in a dose-dependent manner as they are known to store xenobiotics like ATR (Icely and Nott, 1992). This morphology deviates from normal morphology, which has been described by Desouky et al. (2013) as having a microvillar brush border lining the lumen of the lobules, small lipid granules and very few vacuoles. The description for “normal hepatopancreas” is similar to what we visualized in crayfish treated with 0 ppb ATR for 10 days (Fig. 1A). Stara et al. (2018) also examined crayfish (*Cherax destructor*) hepatopancreas tissues following a 14-day exposure to 6.86 and 1210 ppb ATR. They did not see any ATR-induced damage following an exposure to 6.86 ppb; however, they found that following the exposure to 1210 ppb, hepatopancreatic tissue displayed disintegration of the epithelium and vacuolization. It should be noted that concentrations above 350 ppb are rarely encountered in the environment. Our study showed similar morphological changes occurred following ATR exposure; however, we found that these changes can occur at exposure concentrations as low as 10 ppb. These effects on morphology also increase in a dose-dependent manner.

In addition to causing changes in the morphology of the hepatopancreas lobules, ATR-induced DNA damage also occurred in cells of the hepatopancreas in a dose-dependent manner post exposure (see Fig. 2). We found a significant increase in the percentage of cells that were TUNEL positive and

presumably apoptotic following a 10-day ATR exposure to 100 and 300 ppb. ATR exposure has been shown to cause DNA damage in the liver and hepatopancreas of other aquatic organisms. For example, when streaked prochilod (*P lineatus*) received an acute (48 h) ATR exposure of 10 ppb ATR, they displayed a significant increase in DNA damage following a comet assay (Santos and Martinez, 2012). Zhu et al. (2011b) also showed that when zebrafish were exposed to ATR ranging from 10 to 1000 ppb for 5 to 25 days, there was a significant increase DNA damage. DNA damage was also seen in olfactory sensory neurons of crayfish (*F. virilis*), erythrocytes of goldfish (*Carassius auratus*) and Nile tilapia (*Oreochromis niloticus*) and blood and gill cells of streaked prochilod fish following environmentally relevant ATR exposures (de Campos-Ventura et al., 2008; Cavas, 2011; Santos and Martinez, 2012; Abdulelah et al., 2020). Overall, ATR-induced alterations of tissue morphology and DNA damage may lead to functional changes in the tissues affected.

Physiological and biochemical changes have also been noted in hepatopancreas and liver tissues post-ATR exposure. For example, change in biochemical profiles in crayfish were observed following ATR exposures. These include increases in antioxidant biomarkers (catalase activity and glutathione reductase) as well as changes in the expression and activity of cytochrome P450 and glutathione-S-transferase, post-exposure (Stara et al., 2018; Awali et al., 2019). Santos and Martinez (2012) also showed that acute ATR exposures in streaked prochilod led to decreases in antioxidant and biotransformation enzymes. Similar changes were noted in zebrafish (Zhu et al., 2011a; Zhu et al., 2011b). Alterations in physiology may be caused by the changes in the histopathology of the hepatopancreas or liver tissue and its subsequent inability to function properly. Further, reallocating energy resources for cell and tissue repair as well as detoxification of ATR and/or other xenobiotics may be detrimental to the animal's long-term health. Overall, because the hepatopancreas serves as the main energy reserve for growth and molting and is the main organ for detoxification, any impairments in this organ could lead to decreased chance of survival and ultimately affect population size.

Conclusions:

Following acute ATR exposures, we visualized marked changes in the morphology of the hepatopancreas. There were increases in degeneration of the tubular epithelium, necrosis of the microvillar brush border and dilation of the lumen. The number of secretory B (blister-like) cells containing vacuoles increased following ATR exposure for all concentrations tested. Furthermore, there was a significant increase in the percentage of cells that contained DNA damage and were presumptively apoptotic in crayfish treated with 100 and 300 ppb ATR, both ecologically relevant ATR concentrations. This is concerning as an overall degeneration of the lobules of the hepatopancreas may lead to long-term changes in physiology as the hepatopancreas is important for growth and molting as well as, digestion, absorption, storage of nutrients and detoxification (Holdich, 2002). These negative physiological changes may in turn negatively impact crayfish growth, development and population size, which may subsequently have cascading detrimental effects on the aquatic ecosystem. In future studies, it is important to determine if ATR-induced cellular damage in the hepatopancreas can be repaired and proper function restored. Moreover, knowledge of the exposure concentrations that cause physiological and

biochemical impairments is important for regulating exposure concentrations and length of exposure. Although the EPA limits ATR concentrations at 15 ppb, we observed morphological changes in the hepatopancreas occurring following a 10 ppb exposure (EPA, 2020).

Abbreviations:

Atrazine - ATR

Declarations:

COMPETING INTEREST:

The authors declare that they have no known competing financial interests or personal relationships that could have appeared to influence the work reported in this paper.

ACKNOWLEDGEMENTS:

The authors thank Dr. Kendra Evans (Department of Chemistry and Biochemistry, University of Detroit Mercy) for previous analysis of ATR treatment concentrations and AbdrhmanAlmouseli for help with crayfish treatments and dissections. We are also grateful for statistical support from Dr. Paul Moore (Bowling Green State University) and for the generous support from the Barry Goldwater Scholarship and Excellence in Education (scholarship awarded to S.A.A) and the University of Detroit Mercy (Faculty Research Award to R.M.B.).Work reported in this publication was supported by the National Institutes of Health Common Fund and Office of Scientific Workforce Diversity under three linked awards RL5GM118981, TL4GM118983, and 1UL1GM118982 administered by the National Institute of General Medical Sciences.

References:

1. Abd El-Atti, M., Desouky, M., Mohamadien, A., Said, R., 2019. Effects of titanium dioxide nanoparticles on red swamp crayfish, *Procambarus clarkii*: Bioaccumulation, oxidative stress and histopathological biomarkers. The Egyptian Journal of Aquatic Research 45, 11-18.
2. Abdulelah, S., Crile, K., Almouseli, A., Awali, S., Tutwiler, A., Tien, E., Manzo, V., Hadeed, M., Belanger, R., 2020. Environmentally relevant atrazine exposures cause DNA damage in cells of the lateral antennules of crayfish (*Faxonius virilis*). Chemosphere 239.
3. Al-Sawafi, A., Yan, Y., 2013. Bioconcentration and antioxidant status responses in zebrafish (*Danio rerio*) under atrazine exposure. International Journal of Chemical Engineering and Applications 4, 204.
4. Awali, S., Abdulelah, S., Crile, K., Yacoo, K., Almouseli, A., Torres, V., Dayfield, D., Evans, K., Belanger, R., 2019. Cytochrome P450 and Glutathione-S-transferase activity are altered following environmentally

relevant atrazine exposures in crayfish (*Faxonius virilis*). Bulletin of Environmental Contamination and Toxicology 103, 579-584.

5. Bancroft, J., Stevens, A., 1990. Theory and practice of histological techniques. 3 ed. Churchill Livingstone, New York.
6. Bates, D., Mächler, M., Bolker, B., Walker, S., 2015. Fitting linear mixed-effects models using lme4. Journal of Statistical Sofware 67, 1-48.
7. Bautista, F., Junior, A., Corcini, C., Acosta, I., Caldas, S., Primel, E., Zanette, J., 2018. The herbicide atrazine affects sperm quality and the expression of antioxidant and spermatogenesis genes in zebrafish testes. Comparative Biochemistry and Physiology Part C: Toxicology & Pharmacology 206, 17-22.
8. Belanger, R., Evans, K., Abraham, N., Barawi, K., 2017a. Diminished conspecific odor recognition in the rusty crayfish (*Orconectes rusticus*) following a 96-h exposure to atrazine. Bulletin of Environmental Contamination and Toxicology 99, 555-560.
9. Belanger, R.M., Lahman, S.E., Moore, P.A., 2017b. Crayfish, an experimental model for
10. examining exposure to environmental contamination., in: Larramendy, M.L. (Ed.), Ecotoxicology and Genotoxicology: Non-Traditional Aquatic Models, Royal Society of Chemistry, Cambridge, UK, pp. 124-156.
11. Belanger, R.M., Mooney, L.N., Nguyen, H.M., Abraham, N.K., Peters, T.J., Kana, M.A., May, L.A., 2016. Acute atrazine exposure has lasting effects on chemosensory responses to food odors in crayfish (*Orconectes virilis*). Arch Environ Contam Toxicol 70, 289-300.
12. Brown, B., 1982. The form and function of metal-containing 'granules in invertebrate tissues. Biological Reviews 57, 621-667.
13. Brzezicki, J.M., Andersen, M.E., Cranmer, B.K., Tessari, J.D., 2003. Quantitative identification of atrazine and its chlorinated metabolites in plasma. Journal of Analytical Toxicology 27, 569-573.
14. Cavas, T., 2011. In vivo genotoxicity evaluation of atrazine and atrazine–based herbicide on fish *Carassius auratus* using the micronucleus test and the comet assay. Food and Chemical Toxicology 49, 1431-1435.
15. Comber, S.D.W., 1999. Abiotic persistence of atrazine and simazine in water. Pesticide Science 55, 696-702.
16. de Albuquerque, F., de Oliveira, J., Moschini-Carlos, V., Fraceto, L., 2020. An overview of the potential impacts of atrazine in aquatic environments: Perspectives for tailored solutions based on nanotechnology. Science of The Total Environment 700, 1-9.
17. de Campos-Ventura, B., de Fransceschi de Angelis, D., Marin-Morales, M., 2008. Mutagenic and genotoxic effects of the Atrazine herbicide in *Oreochromis niloticus* (Perciformes, Cichlidae) detected by the micronuclei test and the comet assay. Pesticide Biochemistry and Physiology 90, 42-51.
18. Desouky, M.M.A., Abdel-Gawad, H., Hegazi, B., 2013. Distribution, fate and histopathological effects of ethion insecticide on selected organs of the crayfish, *Procambarus clarkii*. Food and Chemical Toxicology 52, 42-52.

19. du Preez, H., Van Vuren, J., 1992. Bioconcentration of atrazine in the banded tilapia, *Tilapia sparrmanii*. Comparative Biochemistry and Physiology. C, Comparative Pharmacology and Toxicology 101, 651-655.
20. EPA, 2014. Atrazine updates: 2014 atrazine ecological exposure monitoring program data, United States Environmental Protection Agency.
21. EPA, 2020. Atrazine: Interim Registration Review Decision Environental Protection Agency Case Number 0062 1-57.
22. Flynn, K., Wedin, M.B., Bonventre, J.A., Dillon-White, M., Hines, J., Weeks, B.S., Andre, C., Schreibman, M.P., Gagne, F., 2013. Burrowing in the freshwater mussel *Elliptio complanata* is sexually dimorphic and feminized at low levels of atrazine. Journal of Toxicology and Environmental Health-Part a-Current Issues 76, 1168-1181.
23. Giddings, J., 2005. Atrazine in North American surface waters: A probabilistic aquatic ecological risk assessment. SETAC.
24. Graymore, M., Stagnitti, F., Allinson, G., 2001. Impacts of atrazine in aquatic ecosystems.
25. Environment International 26, 483-495.
26. Gunkel, G., Streit, B., 1980. Mechanisms of bioaccumulation of a herbicide (atrazine, s-triazine) in a freshwater mollusc (*Ancylus fluviatilis müll.*) and a fish (*Coregonus fera jurine*). Water Research 14, 1573-1584.
27. Hayes, T., Haston, K., Tsui, M., Hoang, A., Haeffele, C., Vonk, A., 2003. Atrazine-induced hermaphroditism at 0.1 ppb in American leopard frogs (*Rana pipiens*): Laboratory and field evidence. Environmental Health Perspectives 111, 568-575.
28. Heisler-Taylor, T., Kim, B., Reese, A., Hamadmad, S., Kusibati, R., Fischer, A., Cebulla, C., 2018. A new multichannel method quantitating TUNEL in detached photoreceptor nuclei. Experimental Eye Research 176, 121-129.
29. Holdich, D.M., 2002. Biology of Freshwater Crayfish. Oxford: Blackwell Science, New York, NY.
30. Icely, J.D., Nott, J.A., 1992. Digestion and absorption: digestive system and associated organs. Microscopic Anatomy of Invertebrates 10, 147-201.
31. Jablonowski, N.D., Schaffer, A., Burauel, P., 2011. Still present after all these years: persistence plus potential toxicity raise questions about the use of atrazine. Environmental Science and Pollution Research 18, 328-331.
32. Jacomini, A., Avelar, W., Martinêz, A., Bonato, P., 2006. Bioaccumulation of atrazine in freshwater bivalves *Anodontites trapesialis* (Lamarck, 1819) and *Corbicula fluminea* (Müller, 1774). Archives of Environmental Contamination and Toxicology 51, 387-391.
33. Koutnik, D., Stara, A., Zuskova, E., Kouba, A., Velisek, J., 2014. The effect of subchronic metribuzin exposure to signal crayfish (*Pacifastacus leniusculus* Dana 1852). Neuro Endocrinol Lett 35 Suppl 2, 51-56.

34. Kuznetsova, A., Brockhoff, P., Christensen, R., 2017. lmerTest package: tests in linear mixed effects models. Journal of Statistical Software 82, 1-26.
35. Laurenz, J., Lietz, L., Brendelberger, H., Lehmann, K., Georg, A., 2020. Noble crayfish are more sensitive to terbuthylazine than parthenogenetic marbled crayfish. Water, Air, & Soil Pollution 231, 1-11.
36. LeBlanc, R., Brown, R., FitzGibbon, J., 1997. Modeling the effects of land use change on the water temperature in unregulated urban streams. Journal of Environmental Management 49, 445-469.
37. Liu, X.M., Shao, J.Z., Xiang, L.X., Chen, X.Y., 2006. Cytotoxic effects and apoptosis induction of atrazine in a grass carp (*Ctenopharyngodon idellus*) cell line. Environmental Toxicology 21, 80-89.
38. Muñoz de Toro, M., Maffini, M., Giardina, R., Luque, E., 1998. Processing fine needle aspirates of prostate carcinomas for standard immunocytochemical studies and *in situ* apoptosis detection. Pathology-Research and Practice 194, 631-636.
39. Popescu-Marinescu, V., Manolache, V., Nastasescu, M., Marinescu, C., 1997. Structural modifications induced by cooper in *Astacus leptodactylus* (Crustacea, Decapoda) hepatopancreas. Rom. J. Biol. Sci 1, 99-105.
40. Santos, T., Martinez, C., 2012. Atrazine promotes biochemical changes and DNA damage in a Neotropical fish species. Chemosphere 89, 1118-1125.
41. Solomon, K.R., Carr, J.A., Du Preez, L.H., Giesy, J.P., Kendall, R.J., Smith, E.E., Van Der Kraak, G.J., 2008. Effects of Atrazine on Fish, Amphibians, and Aquatic Reptiles: A Critical Review. Critical Reviews in Toxicology 38, 721-772.
42. Stara, A., Kouba, A., Velisek, J., 2018. Biochemical and histological effects of sub-chronic exposure to atrazine in crayfish *Cherax destructor*. Chemico-Biological Interactions 291, 95-102.
43. Stara, A., Kubec, J., Zuskova, E., Buric, M., Faggio, C., Kouba, A., Velisek, J., 2019. Effects of S-metolachlor and its degradation product metolachlor OA on marbled crayfish (*Procambarus virginalis*). Chemosphere 224, 616-625.
44. Stara, A., Zuskova, E., Kouba, A., Velisek, J., 2016. Effects of terbuthylazine-desethyl, a terbuthylazine degradation product, on red swamp crayfish (*Procambarus clarkii*). Science of The Total Environment 566–567, 733-740.
45. Steele, A., Belanger, R., Moore, P., 2018. Exposure through runoff and ground water contamination differentially impact behavior and physiology of Crustaceans in fluvial systems. Archives of Environmental Contamination and Toxicology 75, 436-448.
46. Tavera-Mendoza, L., Ruby, S., Brousseau, P., Fournier, M., Cyr, D., Marcogliese, D., 2002. Response of the amphibian tadpole (*Xenopus laevis*) to atrazine during sexual differentiation of the testis. Environmental Toxicology and Chemistry 21, 527-531.
47. Team, R.C., 2019. R: A language and environment for statistical computing, In: Computing, R.F.f.S. (Ed.), Vienna, Austria.
48. Tong, S., Chen, W., 2002. Modeling the relationship between land use and surface water quality. Journal of Environmental Management 66, 377-393.

49. Van Der Kraak, G., Hosmer, A., Hanson, M., Kloas, W., Solomon, K., 2014. Effects of atrazine in fish, amphibians, and reptiles: An analysis based on quantitative weight of evidence. Critical Reviews in Toxicology 44, 1-66.
50. Velisek, J., Stara, A., Zuskova, E., Kouba, A., 2017. Effects of three triazine metabolites and their mixture at environmentally relevant concentrations on early life stages of marbled crayfish
51. (*Procambarus fallax f. virginalis*). Chemosphere 175, 440-445.
52. Walther, J.S., 2003. Surface water pesticide contamination in the upper Terrebonne Basin of Louisiana. Master's thesis., Louisiana State University, Baton Rouge, LA, p. 55.
53. Wei, K., Yang, J., 2015. Oxidative damage of hepatopancreas induced by pollution depresses humoral immunity response in the freshwater crayfish *Procambarus clarkii*. Fish & Shellfish Immunology 43, 510-519.
54. Xiao, X., Han, D., Zhu, X., Yang, Y., Xie, S., Huang, Y., 2014. Effect of dietary cornstarch levels on growth performance, enzyme activity and hepatopancreas histology of juvenile red swamp crayfish, *Procambarus clarkii* (Girard). Aquaculture 426, 112-119.
55. Xing, H., Wang, X., Sun, G., Gao, X., Xu, S., Wang, X., 2012. Effects of atrazine and chlorpyrifos on activity and transcription of glutathione S-transferase in common carp (*Cyprinus carpio* L.). Environmental Toxicology and Pharmacology 33, 233-244.
56. Zhu, L.-S., Shao, B., Song, Y., Xie, H., Wang, J., Wang, J.-H., Liu, W., Hou, X.-X., 2011a. DNA damage and effects on antioxidative enzymes in zebra fish (*Danio rerio*) induced by atrazine. Toxicology Mechanisms and Methods 21, 31-36.
57. Zhu, L.S., Dong, X.L., Xie, H., Wang, J., Wang, J.H., Su, J., Yu, C.W., 2011b. DNA damage and effects on glutathione-S-transferase activity induced by atrazine exposure in zebrafish (*Danio rerio*). Environmental Toxicology 26, 480-488.
58. Zuur, A., Ieno, E., Walker, N., Saveliev, A., Smith, G., 2009. Mixed effects models and extensions in ecology with R. Springer Science & Business Media, New York.

Figures

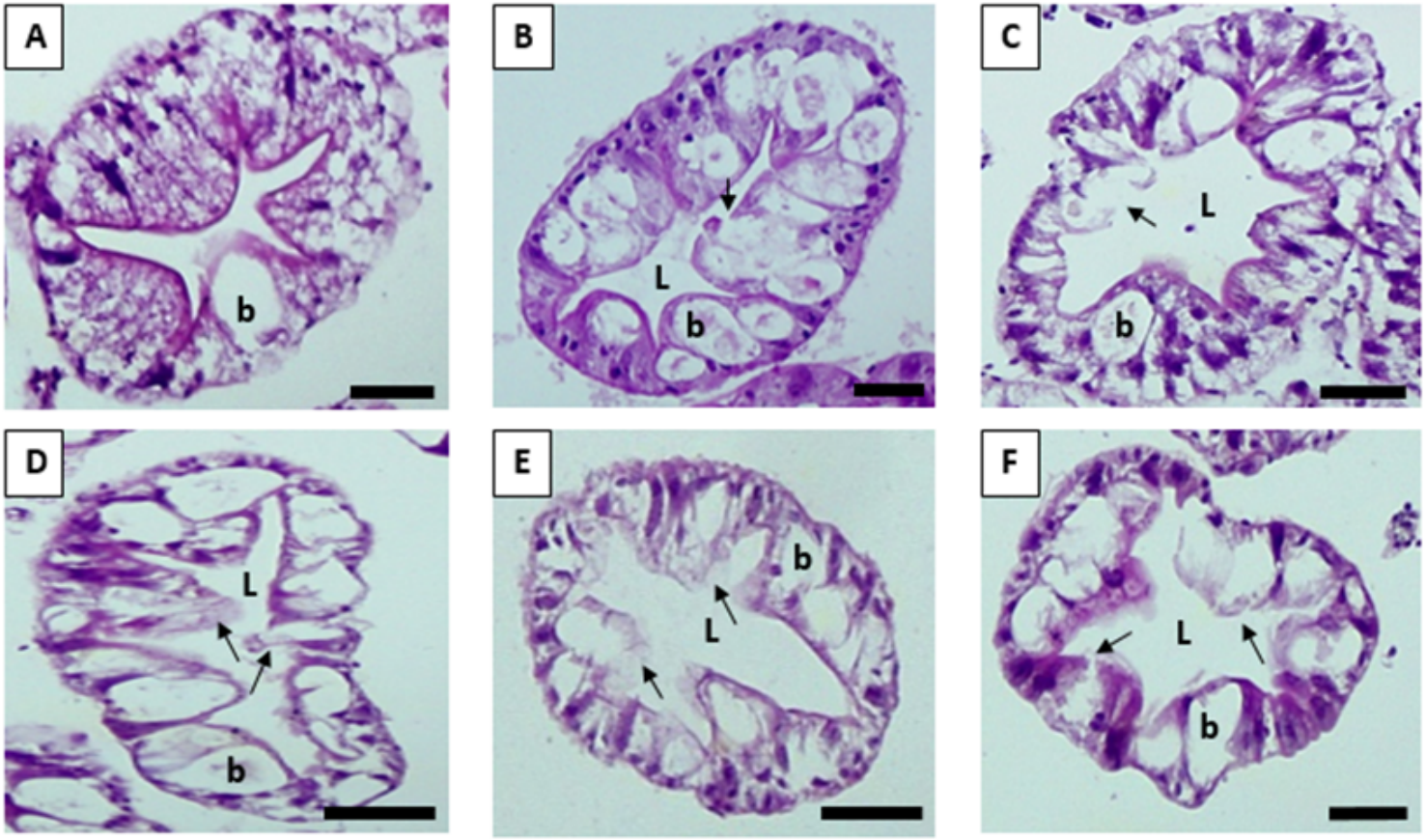

Figure 1

H&E histology of transverse sections through the hepatopancreas of crayfish following a 10-day exposure to ATR. A: 0 ppb, B: 10 ppb, C: 40 ppb, D: 80 ppb, E: 100 ppb, F: 300 ppb. Secretory B (blister-like) cells (b) containing single large secretory vesicles (vacuoles) increased in number as ATR exposure concentration increased. Tubule lumen (L) dilation was also observed following ATR exposures above 40 ppb. Necrosis of microvilli brush border and membrane degeneration was visualized in hepatopancreas lobules post-ATR exposure (arrows). Scale bar is 50 µm.

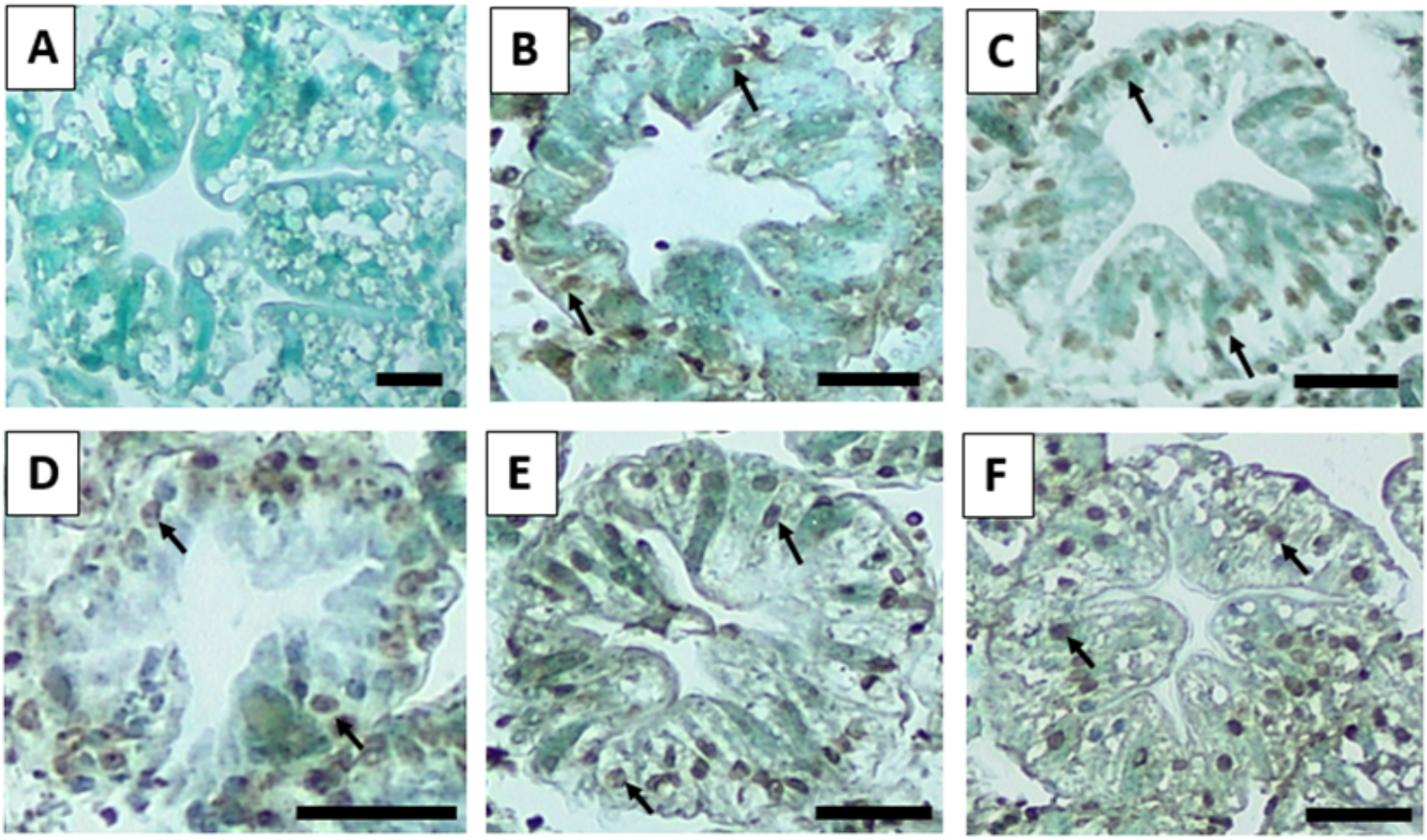

Figure 2

Light micrographs of transverse sections of TUNEL-labeled hepatopancreas tissue following a 10-day exposure to ATR. A: 0 ppb, B: 10 ppb, C: 40 ppb, D: 80 ppb, E: 100 ppb, F: 300 ppb. Increases in TUNEL-positive cells can be seen following ATR exposures of 10 ppb and above (arrows). Scale bar is 50 µm.

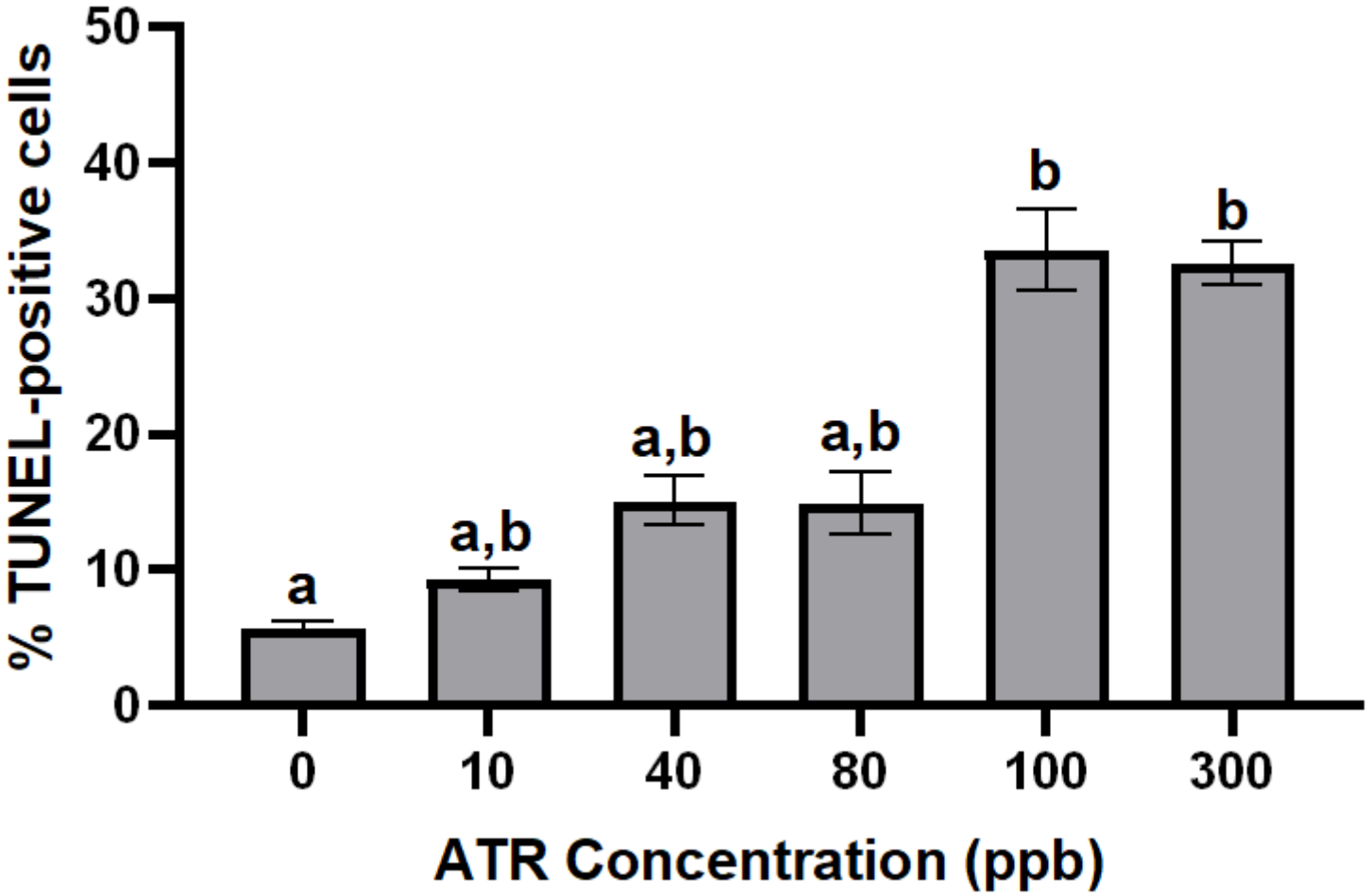

Figure 3

Percentage of TUNEL-positive cells in the hepatopancreas of crayfish following a 10-day exposure to 0, 10, 40, 80, 100 and 300 ppb ATR. Percent TUNEL-positive cells are present in all concentrations tested, but increased significantly at exposure concentrations of 100 ppb ATR and above. Control and ATR-treated groups are assigned different letters a, b when they are significantly different ($p < 0.01$).

Supplementary Files

This is a list of supplementary files associated with this preprint. Click to download.

- GA.png